JOURNAL OF MATERIALS SCIENCE 28 (1993) 3983–3990

Fracture mechanics of short glass fibre-reinforced nylon composite

S. HASHEMI, J. MUGAN
The University of North London, London School of Polymer Technology, Holloway Road, London N7 8DB, UK

The fracture behaviour of injection-moulded short glass fibre-reinforced, thermoplastic nylon 6.6 plaques has been studied under static loading using compact tension specimens and under impact loading using single-edge notched charpy specimens. The influences of specimen position as taken from the plaque mouldings, notch direction, notch sharpness and the rate of testing on the fracture toughness of this composite system were investigated. Results indicated that the fracture toughness is highest for the cracks perpendicular to the mould fill direction and is lowest for cracks parallel to the mould fill direction. A single fracture parameter, K_c, seems to be inadequate for fracture toughness characterization. Evaluation of the fracture toughness as a function of notch sharpness indicated that for notches perpendicular to the mould fill direction the fracture toughness is not affected by the sharpness of the initial notch. However, for cracks in the mould fill direction, sharpness of the initial notch had a significant effect upon the measured value of the fracture toughness. Results also indicated, that the fracture toughness is rate insensitive over the crosshead speed ranging from 0.5–50 mm min^{-1}. Finally, the specimen position, as taken from plaque mouldings, had no significant effect on the measured value of the fracture toughness.

1. Introduction

The use of short fibre-reinforced thermoplastic composites in engineering applications is both growing and diversifying. However, when they are injection moulded, they are among the most complex of composite materials. In their final moulded form, they are typified by misaligned arrays of fibres of various lengths dispersed in a viscoelastic matrix. The orientation of the short fibres is determined by the flow characteristics of the melt, which in turn depend on the mould geometry, the wall thickness of the final parts, the processing conditions and the length and fraction of fibres in the composite. Short-fibre composite components manufactured by the injection-moulding processes are highly anisotropic and inhomogeneous at all levels of fibre content. In addition, the alignment of the fibres is very complex. Generally, fibres near the outer surfaces will be aligned in the mould fill direction due to a converging stress field during injection moulding, while fibres near the centre of the moulding will be aligned at right angles to the mould fill direction due to the diverging stress field during moulding. Previous studies [1–3] have shown that the overall fibre alignment depends upon the ratio of skin to core, and this is influenced by the thickness of the moulding and its geometry. For example, in thin injection-moulded plaques, the skin is strongly dominant, whereas for any plaque more than about 6 mm thick, skin layers seem to reach a fixed thickness and above this limit the core contributes more to the cross-section of the plaques than the sum of the two skin layers. Furthermore, it is shown [1] that increasing the weight fraction of fibres, increases the thickness of the centre layer (core), increases the degree of fibre orientation in the individual layers and finally, increases the difference between the orientation of centre and the surface layers.

One of the crucial problems of the injection-moulded short-fibre composites is how the fibre orientation influences their fracture behaviour and whether a single linear elastic fracture mechanics (LEFM) parameter, such as fracture toughness, K_c, or the strain energy release rate, G_c, can be adequate in describing the material toughness. The purpose of this investigation is to determine the effects of fibre orientation, crack length, notch sharpness, specimen size and the rate of testing upon fracture toughness of glass short fibre-reinforced nylon 6.6.

2. Experimental procedure

2.1. Material and moulding

The composite comprised short E-glass fibres dispersed in a thermoplastic nylon 6.6 matrix. The material was supplied as injection-moulded end-gated rectangular plaques of dimensions 100 mm × 254 mm × 3.2 mm. Plaques contained 33% by volume of short E-glass fibres.

The injection mouldings of fibre-reinforced nylon will be anisotropic and inhomogeneous. The alignment of the fibres will be complex. Previous investigations [1] have shown that in 3.2 mm thick

0022–2461

injection-moulded plaques, the fibres near the mould surface are aligned predominantly in the mould fill direction and the sum of the thickness of the two surface layers is approximately 75% of the plaque thickness. Because the same mould geometry and thickness were used for all specimens, we therefore assume that skin dominates the fibre orientation. Consequently, when specimens are cut at 0° or 90° to the mould fill direction we may regard them as along or across the predominant fibre direction.

2.2. Fracture tests

2.2.1. Static loading

Fracture toughness tests were conducted with compact tension specimens (see Fig. 1) on an Instron testing machine. The initial notches were prepared by first forming saw-cut slots which were then sharpened with a razor blade. The razor blade was mounted on a laboratory attachment so that penetration could be controlled carefully. The fresh edge of a razor blade was then pushed through the material slowly to a depth of about 2 mm. The notch lengths were measured using a travelling microscope. The majority of the specimens were fractured at room temperature at a constant crosshead speed of 5 mm min^{-1} and the load–displacement trace for each specimen was recorded.

Fracture tests were conducted in order to investigate the effect of the following on the fracture toughness: crack length, specimen size (effect of the specimen width), specimen position as taken from the plaque mouldings, sharpness of the initial crack, crack direction with respect to the mould fill direction, and rate of testing.

2.3. Impact tests

Charpy impact tests were carried out on single-edge notched three-point bend specimens (see Fig. 2). Specimens were 10 mm wide and the span to depth ratio, L/D, was set at 4:1. The initial notches were prepared as before and all the specimens were impacted at room temperature at a hammer speed of 3 m s^{-1}.

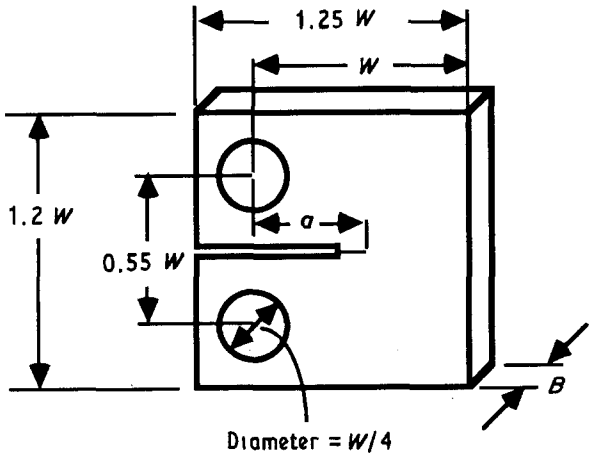

Figure 1 Compact tension specimen configuration: $W = 40$ mm, $B = 3.2$ mm.

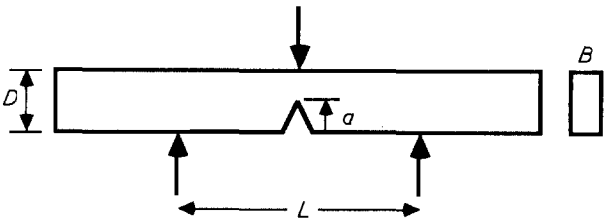

Figure 2 Charpy impact specimen.

3. Data analysis

The theory of linear elastic fracture mechanics (LEFM) is concerned with crack initiation occurring at nominal stresses that are well below the uniaxial yield stress of the material. Tests on pre-cracked specimens undergoing little plastic deformation are carried out to measure the fracture toughness, K_c, which characterizes the elastic field around the crack tip.

To evaluate the fracture toughness, K_c, use is made of the standard relation for isotropic materials [4]

$$K_c = Y(a/W)\sigma_c a^{1/2} \quad (1)$$

where $Y(a/W)$ is a geometrical correction factor, σ_c is the gross applied stress, and a is the initial crack length. For the compact tension specimen (CTEN), the geometrical correction factor is given by

$$Y(x) = \left(\frac{1}{x^{1/2}}\right)\left[\frac{2 + x}{(1 - x)^{3/2}}\right](0.886 + 4.64x - 13.32x^2 + 14.72x^3 - 5.6x^4) \quad (2)$$

where $x = a/W$. Because fracture processes are controlled by stresses and strains at the tip of the crack, and the states of triaxial stresses near the crack tip of a specimen are influenced greatly by specimen size, the fracture parameter, K_c, is therefore expected to vary with the size of specimen used. The material toughness is best characterized by its value under plane-strain conditions, K_{c1}, and to achieve this state of stress the specimen dimensions must exceed some multiple of the plastic zone size, R_p. This limitation on the specimen size forms the basis of the minimum test-piece size requirements of the ASTM E-399 standard for K_{c1} determination [5], i.e.

$$B \geqslant 2.5\left(\frac{K_{c1}}{\sigma_y}\right)^2 \quad (3a)$$

$$W \geqslant 2B \quad (3b)$$

where B and W are the specimen thickness and width respectively and σ_y is the uniaxial yield stress of the material. K_c (or K_{c1}) is related to the energy per unit area of the fracture G_c (or G_{c1} for plane strain fracture) known as strain energy release rate by the following relationship

$$K_c^2 = E^* G_c \quad (4)$$

where E^* is the effective modulus of elasticity ($= E$ for plane stress, $E/(1 - \nu^2)$ for plane strain, where ν is the Poisson's ratio). The elastic modulus, E^*, can be calculated from the compliance of the notched specimens. The load-line compliance and the stress intensity factor are related according to

$$\left(\frac{K_I B W^{1/2}}{P}\right)^2 = \frac{1}{2} E^* B \frac{dC}{dx} \quad (5)$$

where $C = \delta/P$ is the load-line compliance and K_I is the Mode I stress intensity factor. Substituting $K_I = \sigma Y a^{1/2}$ and $\sigma = P/(BW)$ into Equation 5 we obtain

$$Y^2(x)x = \frac{1}{2}E^*B\frac{dC}{dx} \quad (6)$$

hence

$$C = C_0 + \frac{2}{E^*B}\int_0^x Y^2(x)x\,dx \quad (7)$$

where C_0 is the compliance of the non-cracked specimen [6]. Rearranging Equation 7 gives

$$E^* = \frac{F(x)}{CB} \quad (8)$$

where $F(x)$ is a function containing the x terms. Entering the values of $F(x)$ and the inverse slope of the load–displacement records (i.e. compliance, C) into Equation 8 produces the value of E^* which may now be used to relate K_c to G_c via Equation 4.

Linear elastic fracture mechanics have also been used extensively to study fracture under impact loading. Under impact, the strain energy release rate, G_c, is determined directly from the measured fracture energies. The strain energy, U, per unit thickness, absorbed in deflecting a cracked elastic test piece of thickness, B, and depth, D, is related to the critical value of strain energy release rate, G_c, by the following equation

$$U = G_c BD\phi + U_k \quad (9)$$

where U_k is the kinetic energy of the broken specimen halves, BD is the cross-sectional area and ϕ is the compliance calibration factor which is a function of specimen geometry and notch dimensions. For single-edge notch three-point bend specimens, ϕ is given by

$$\phi = \frac{\int Y^2(x)x\,dx}{Y^2(x)x} + \frac{L}{18DY^2(x)x} \quad (10)$$

where $x = a/D$ and $Y(x)$ is determined from the expression 4

$$Y(x) = 1.93 - 3.07x + 14.53x^2 - 25.11x^3 + 25.8x^4 \quad (11)$$

According to Equation 9, strain energy release rate may be determined from the slope of line U versus $BD\phi$. The positive intercept, U_k, on the energy axis gives the energy losses which do not contribute to fracture of the specimen (e.g. kinetic energy loss in the specimens).

4. Results and discussion

4.1. Effect of crack length on fracture toughness

To examine the effect of crack length on fracture stress and fracture toughness, several compact tension specimens of $W = 40$ mm were prepared from the position B on the plaque mouldings as shown in Fig. 3. All the notches were inserted parallel to the mould fill direction using the razor blade and all the specimens were fractured at a crosshead speed of 5 mm min^{-1}.

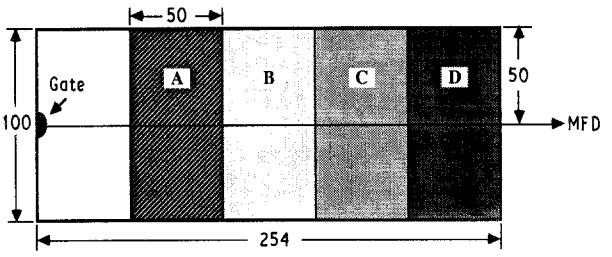

Figure 3 Specimen positions as coded in this study.

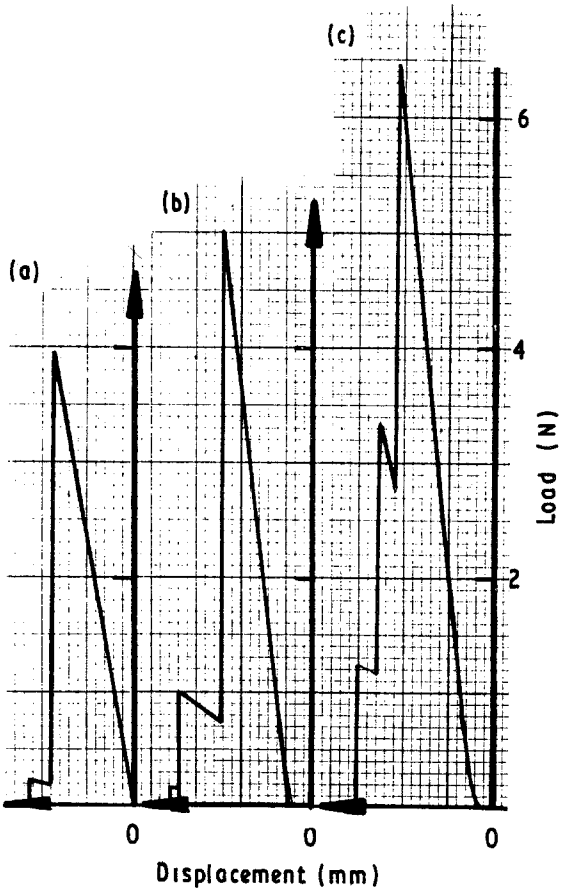

Figure 4 Typical load–displacement curves for several a/W ratios: (a) 0.5, (b) 0.4 and (c) 0.30.

Fig. 4 shows typical load versus displacement curves for varying crack lengths. The load–displacement curves are seen to be almost linear until the maximum load, P_c, is reached. At the maximum load the crack in the specimen began to grow unstably in the mould fill direction before being arrested. As indicated by the curves, the presence of the notches leads to a reduction of strength. This reduction in the composite strength is for two reasons; firstly, the effective cross-sectional area of the specimen is reduced to $(W - a)B$ and secondly, stress concentrations are produced at the notch tips.

From the plot of the net section stress, $\sigma_n = P_c/[(W - a)B]$ against the crack length, a (see Fig. 5), it is apparent that the net section stress is dependent upon the notch depth, thus indicating that the composite is notch sensitive (we show later that the composite strength is also strongly dependent on the notch sharpness).

The fracture toughness, K_c, is defined as the value of the stress intensity factor, K_I, at which the crack in the

specimen began to grow unstably before being arrested. This occurred at the maximum load, P_c, as mentioned earlier. To test the applicability of LEFM theory, a plot of $(\sigma_c/Y)^2$ versus $1/a$ was constructed as shown in Fig. 6. According to Equation 1 this plot should be linear, passing through the origin with a slope of K_c^2. From Fig. 6 it is apparent that the experimental data provide a good fit to the LEFM theory as stated by Equation 1 thus indicating that the fracture toughness value measured for this material is almost independent of crack length, which must be seen as a verification of the applicability of linear elastic fracture mechanics concepts to this composite material.

4.2. Effect of the specimen position on fracture toughness

The effect of specimen position (relative to the gate) on the fracture toughness was investigated by dividing the injection-moulded plaques into four areas designated A, B, C and D (see Fig. 3). Four compact tension specimens for each position was prepared (i.e. two from each plaque). All the specimens were razor notched to $a/W \approx 0.3$ in the mould fill direction. Specimens were subsequently fractured at a constant crosshead speed of 5 mm min^{-1}. From the initial length of the crack and the maximum load, a fracture toughness value was calculated for each specimen as shown in Table I. It is evident from data, that the fracture toughness does not vary significantly with position of the specimens as taken from the plaque mouldings. Additional information obtained from Table I indicates that the fibre orientation does not change significantly through the thickness direction from one place to another. The average fracture toughness value for 3.2 mm thick plaques with notches parallel to the mould fill direction as determined from Table I is 6.00 ± 0.17 MPa m$^{1/2}$.

In addition, a mineral content test (ash test) between samples from both ends of the plaques was also carried out to establish the effect of packing on the fibre volume fraction. Results obtained further complimented the above results by indicating a fibre volume difference of only 0.5%.

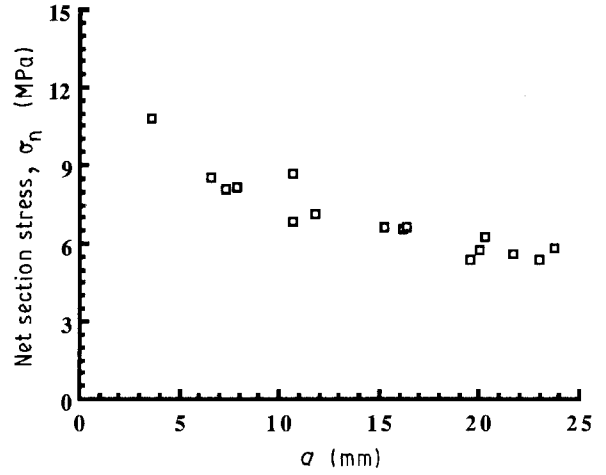

Figure 5 Net section stress versus crack length.

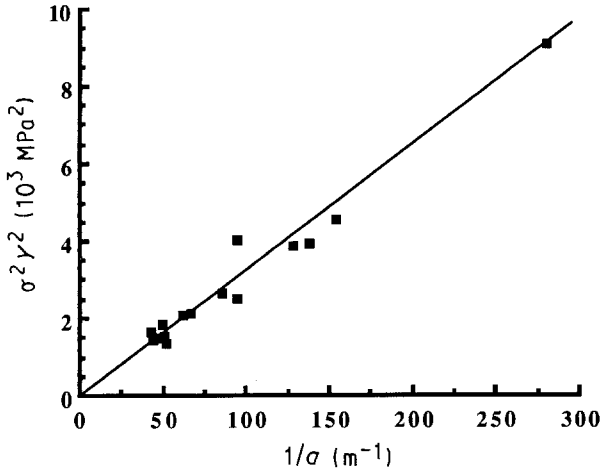

Figure 6 Fracture data for CTEN specimens. $K_c = 5.72$ MPa m$^{1/2}$.

4.3. Effect of the specimen size on fracture toughness

To obtain a valid measurement of the critical stress intensity factor, K_c, several criteria have to be met. Essentially, the effect of specimen thickness, B, the specimen width, W, and the degree of nonlinearity of the load versus deflection trace must all be considered.

4.3.1. Thickness effect

The effect of the specimen thickness, B, of the specimen arises because of the state of stress near the crack tip varies from plane stress in the surface regions of a relatively thick specimen, or throughout the thickness of a thin specimen, to plane strain in the centre of a thick specimen. The stress at which a material yield is greater in a triaxial stress field (plane strain) than in

TABLE I Effect of specimen position on the fracture toughness ($W = 40$ mm)

Position	Crack length (mm)	Fracture stress (MPa)	Fracture toughness (MPa m$^{1/2}$)	Average (MPa m$^{1/2}$)
A	0.31	4.98	5.72	
	0.31	5.40	6.26	
	0.35	5.07	6.42	
	0.27	5.69	5.89	
				6.07 ± 0.32
B	0.30	5.53	6.27	
	0.27	5.50	5.69	
	0.32	4.74	5.42	
	0.25	5.84	5.69	
				5.77 ± 0.36
C	0.23	5.99	5.56	
	0.34	4.68	5.85	
	0.23	6.91	6.38	
	0.26	5.30	5.40	
				5.80 ± 0.43
D	0.27	6.31	6.56	
	0.27	7.02	6.02	
	0.27	5.19	5.55	
	0.28	6.21	6.25	
				6.10 ± 0.43

biaxial stress field (plane stress): the former is a more constrained case and therefore a less extensive degree of plasticity is developed at the crack tip, and lower toughness is observed. Hence, the thickness, B, of the specimen must be sufficiently large to ensure that the state of stress at the tip of the crack is plane strain. Plane strain fracture results in the minimum value of K_c being measured. The minimum thickness, B_{min}, needed for plane strain conditions to dominate is usually taken to be [5]

$$B_{min} \geqslant 2.5\left(\frac{K_Q}{\sigma_y}\right) \quad (12)$$

where K_Q is the provisional value of the stress intensity factor, but whose validity is not yet established. The value of yield stress, σ_y, for this composite was measured to be 180.6 MPa at the testing rate of 5 mm min^{-1}. At this rate, the average fracture toughness for cracks in the mould fill direction is 6.00 MPa m$^{1/2}$, giving the value of minimum thickness, B_{min}, needed as 2.78 mm. Because the specimen thickness used, B, was 3.2 mm, the condition $B_{min} > B$ is therefore fulfilled. It must be noted that although the effect of specimen thickness on fracture toughness has been demonstrated for polymers and even rubber-toughened polymers [8], in the case of short-fibre composites because of the skin/core morphology, the fibre orientation distribution changes with changes in thickness of the moulding and therefore making it difficult to gather evidence on thickness effect alone.

4.3.2. Specimen width effect

A second condition for a valid measurement of K_c is that

$$W_{min} \geqslant 5\left(\frac{K_Q}{\sigma_y}\right)^2 \quad (13)$$

where W_{min} is the minimum width of the specimen which is needed. This arises from the need to avoid excessive plasticity in the ligament $(W - a)$. If the stress in the ligament approaches the yield stress then the value of critical stress intensity factor that is determined will be underestimated.

The effect of specimen width was studied in detail by testing several compact tension specimens of varying widths. A minimum of three specimens for each width was prepared and razor notched to $a/W = 0.5$ in the mould fill direction. The variation of K_c with the width of the compact tension specimens is shown in Fig. 7 (the values are computed from the maximum load and the original notch length). These results show that width does not influence the critical stress intensity factor and the ASTM width requirement is fulfilled, provided specimen width is greater than 5.56 mm.

4.3.3. Non-linearity of the load–displacement curves

The third requirement that has to be met is that the load versus displacement trace should be essentially linear. The trace may show some degree of non-linearity for a variety of reasons; e.g. due to excessive plasticity occurring at the crack tip, due to inelastic or plastic deformations occurring in the bulk of the specimen or due to slow crack growth prior to the maximum load being attained. If slow crack growth occurs before the maximum load is attained then the value of the critical stress intensity factor for crack initiation based upon the maximum load will be an overestimate of the toughness of the material. These problems may be overcome, at least to a good approximation, by following the arbitrary rule embodied in the ASTM standard for testing metals [5] in which a linear straight line is drawn to determine the initial compliance, C, and a further line is then drawn by increasing the initial compliance by 5%, i.e. $C + 5\%$ as shown in Fig. 8. If the line $C + 5\%$ intersects the load curve then $P_{5\%}$ is found, and this is taken as the load at crack initiation. For the value of K_Q based upon either P_{max} or $P_{5\%}$ to be valid, then the following criteria must be met

$$\frac{P_{max}}{P_{5\%}} \leqslant 1.1 \quad (14)$$

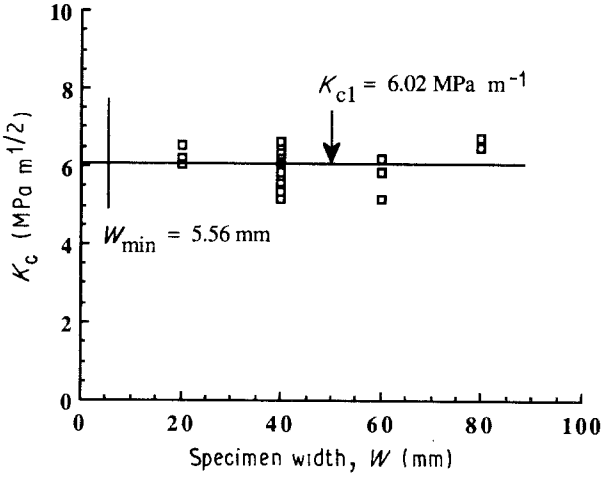

Figure 7 Effect of specimen width on the fracture toughness (L-cracks).

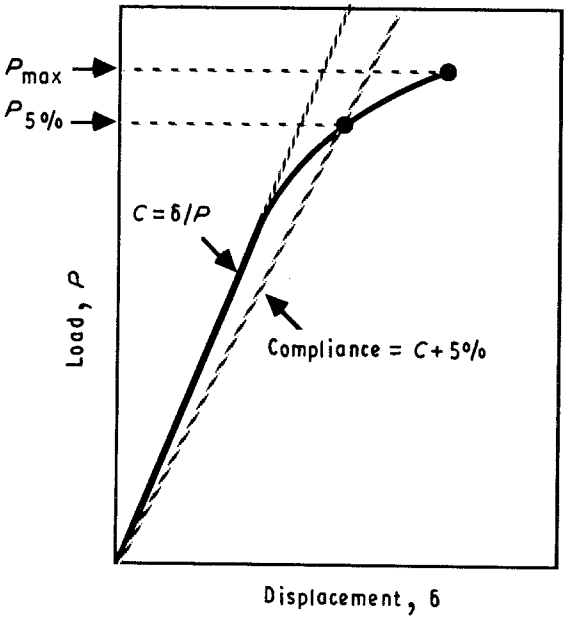

Figure 8 The ASTM 5% offset procedure.

This condition essentially allows 10% non-linearity of the load versus displacement trace before the experimental measurements are declared to be too non-linear for LEFM to apply. Thus, to summarize, if $P_{max}/P_{5\%} > 1.1$ then the test is invalid. If $P_{max}/P_{5\%} < 1.1$ then $P_{5\%}$ is used in the calculation of K_Q, or alternatively P_{max}, if the value falls within two lines.

In the present tests, the load versus displacement traces often exhibited a small degree of non-linearity before the maximum load was reached (see Fig. 4). The intersection of the 5% offset line with the curve was either at the maximum load or immediately after. These analyses suggested that the condition $P_{max}/P_{5\%} < 1.1$ is met and therefore the use of the maximum load for calculating the fracture toughness is fully justified.

From the above analysis we conclude that when the initial notches are in the mould fill direction, the measured fracture toughness value of 6.00 MPa $m^{1/2}$ is indeed the true plane strain value, because all the requirements of ASTM E399 are met.

4.3.4. Effect of crack orientation on fracture toughness

As the fibre alignment yields highly anisotropic mechanical properties, the compact tension specimens were tested in three directions (see Fig. 9): (i) with the initial notch parallel to the melt flow direction (longitudinal direction, L-cracks); (ii) with the initial notch perpendicular to the melt flow direction (transverse direction, T-cracks); and (iii) with the initial notch at 45° to the melt flow direction (cross direction, C-cracks). A minimum of five compact tension specimens with $W = 40$ mm were tested for each crack direction. All the specimens were razor notched to $a/W = 0.50$ and fractured at a constant crosshead speed of 5 mm min^{-1}. The effect of the crack direction on the value of the fracture toughness can be seen from the results given in Table II. The results show a strong dependence of the value of fracture toughness with notch direction. The manner in which specimens were fractured is shown schematically in Fig. 10. In all cases, the crack propagated unstably along the mould fill direction before arresting, thus supporting the view that the fibres are preferentially aligned in the mould fill direction during processing.

When the initial notch was perpendicular to the mould fill direction it was also perpendicular to the fibres and, as a result, the sharp notches became blunted by the presence of the fibres. The stress concentration at the tip of the crack was therefore reduced causing the specimen to fail at a higher fracture stress. This provided greater resistance to crack propagation as reflected by the increase in the K_c value as the notch direction was changed from 0° to 90° with respect to mould fill direction. The ratio of $K_{c,\text{T-cracks}}$ to $K_{c,\text{L-cracks}}$ for this composite is approximately 1.73, and this ratio may change with changes in thickness. Furthermore, as shown in Fig. 10b, c, specimens with T- and C-cracks show large deviations from their initial plane perpendicular to the load direction. For T-cracks, fracture finally occurs in Mode II conditions and for C-cracks it occurs in mixed-mode conditions. Finally, a much higher fracture toughness for T-cracks indicates that the ASTM size criteria (specimen thickness) is not fulfilled and therefore the validity of $K_{c,\text{T-crack}}$ as the plane strain fracture toughness is questionable even though the other conditions were met (i.e. specimen width and the non-linearity).

4.3.5. Effect of notch sharpness on fracture toughness

The effect of the sharpness of the initial notch on fracture toughness was investigated with notches either parallel or perpendicular to the mould fill direction. Sharp notches were formed using razor blade and blunt notches were introduced using saw cuts. All the specimens were notched to $a/W = 0.25$ and fractured at a constant crosshead speed of 5 mm min^{-1}. Results from this study (see Table III) indicated that

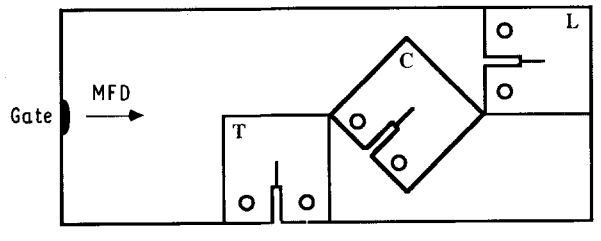

Figure 9 Cracks with respect to plaque geometry (MFD, mould fill direction).

TABLE II Fracture data for CTEN specimens ($W = 40$ mm)

Crack orientation	Fracture toughness (MPa $m^{1/2}$)
L-crack (0°)	6.00 ± 0.17
C-crack (45°)	7.76 ± 0.46
T-crack (90°)	10.36 ± 1.16

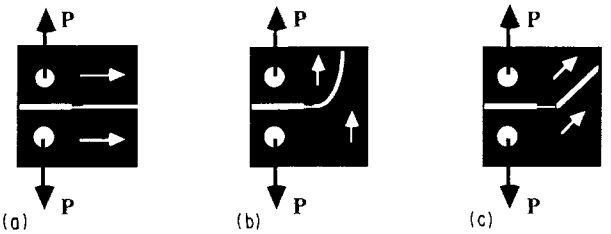

Figure 10 Crack propagation direction in compact tension specimens for: (a) L-cracks, (b) T-cracks and (c) C-cracks. (White arrows show the MFD.)

TABLE III Fracture data for CTEN specimen with $a/W = 0.25$ ($W = 40$ mm)

Crack orientation	Notch sharpness	Fracture toughness (MPa $m^{1/2}$)
L-crack	Razor	6.00 ± 0.17
	Saw cut	7.97 ± 0.41
T-crack	Razor	10.36 ± 1.16
	Saw cut	10.89 ± 1.13

when the initial notches are perpendicular to the mould fill direction, the sharpness of the notch has no significant effect on the measured value of the fracture toughness, because the sharpness is influenced by the presence of the fibres which are preferentially aligned parallel to the mould fill direction. These fibres cause the sharp notch to open up and become blunt and by doing so removing the stress concentration at the tip of the crack. Thus, the material behaviour is almost completely insensitive to the sharpness of the notch and the value of the fracture toughness remains almost unchanged. However, when the initial notch is parallel to the mould direction, the notch remains sharp and consequently the value of the fracture toughness varies with the initial sharpness as borne out by the results of Table III.

4.3.6. Effect of rate on fracture toughness

The effect of testing rate on the fracture toughness was studied over the crosshead speed of 0.5–50 mm min^{-1}. A minimum of four specimens for each rate was prepared and razor notched to $a/W = 0.5$. Notches were inserted either parallel or perpendicular to the mould fill direction. The results obtained from these tests are shown in Table IV. As may be seen there is no significant change in the value of the fracture toughness with the testing rate.

To determine the value of fracture toughness at a higher testing rate, a series of three-point single-edge notched bend specimens were impacted at a speed of 3 m s^{-1}. Fig. 11 shows plots of energy absorbed by the specimen to fracture, U, as a function of $BD\phi$ and, as often observed, these plots show a positive intercept on the U-axis. From the slope of these curves, G_c values of 3.12 kJ m^{-2} for L-cracks and 7.04 kJ m^{-2} for T-cracks were ascertained. It must be noted that under impact, specimens containing T-cracks fractured in Mode I via fibre breakage, as opposed to Mode II, which was the failure mode for this crack configuration under static loading.

To establish the overall effect of rate on G_c, the static values of K_c for L-cracks as given in Table IV were converted into G_c values via the relationship $K_c^2 = E^* G_c$. The elastic modulus, E^*, was calculated by entering the values of $F(x)$ and the compliance, C, into Equation 8. The modulus values calculated for several a/W ratios are given in Table V. These values were obtained from compact tension specimens fractured at a crosshead speed of 5 mm min^{-1} and with notches parallel to the mould fill direction. Furthermore, when a similar analysis was carried out at other rates, the modulus value did not show any significant changes with rate.

Using the average modulus value of 5.36 GPa as obtained from Table V, the K_c values of Table IV were converted into G_c values and this resulted in the G_c versus rate plot of Fig. 12. For T-cracks the static values of K_c cannot be readily converted into G_c values because the failure Mode for T-cracks under static tests was that of Mode II. However, an estimate value of G_c may be ascertained by employing the shear lag analysis which has been used to study axial splitting in continuous, aligned composites [9]. According to the model K_c may be related to G_c by the following relation

$$G_{c,\text{T-cracks}} = \frac{K^2_{c,\text{T-cracks}}}{4E} \quad (15)$$

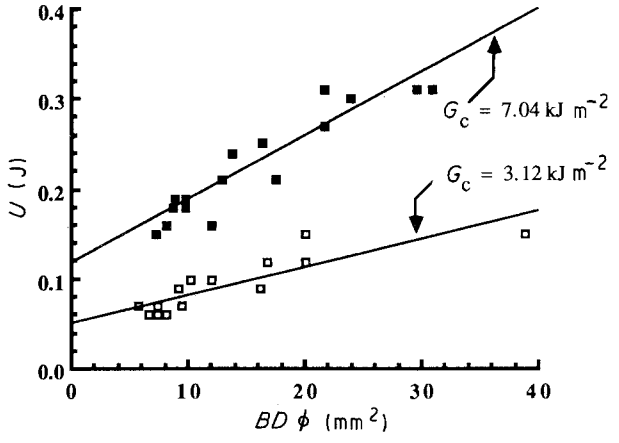

Figure 11 Charpy impact data for (□) L- and (■) T-cracks.

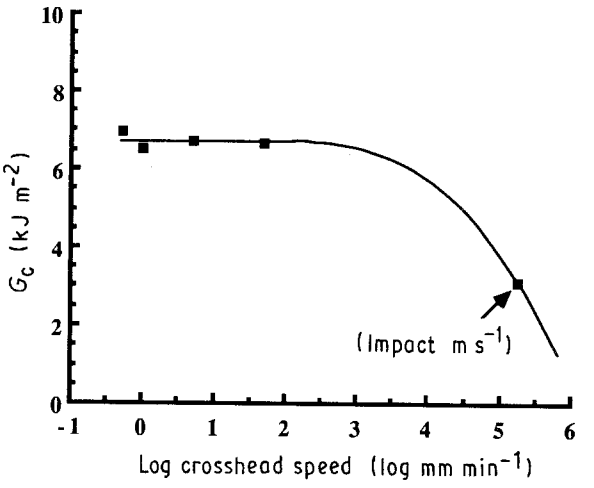

Figure 12 Effect of testing rate on strain energy release rate for L-cracks.

TABLE IV Effect of crosshead speed on the fracture toughness ($B = 3.2$ mm, $W = 40$ mm, $a/W = 0.5$)

Crosshead speed (mm min^{-1})	Fracture toughness (MPa $m^{1/2}$)	
	L-cracks	T-cracks
0.5	6.12 ± 0.40	9.51 ± 0.38
1.0	5.93 ± 0.21	9.41 ± 0.37
5.0	6.00 ± 0.17	10.36 ± 1.16
50.0	5.98 ± 0.35	9.72 ± 0.21

TABLE V Values of C, $F(x)$ and E^* (crosshead speed = 5 mm min^{-1})

$x(=a/W)$	$C(10^{-4}$ mm $N^{-1})$	$F(x)$	E^*(GPa)
0.30	08.48	14.48	5.16
0.40	13.50	23.22	5.38
0.50	22.50	38.00	5.28
0.60	35.25	63.20	5.60

Substituting the average $K_{c,T\text{-cracks}}$ value of 9.75 MPa $m^{1/2}$ and the average modulus value of 5.36 GPa into Equation 15 gives an approximate $G_{c,T\text{-cracks}}$ value of 4.43 kJ m^{-2} for static tests which is considerably lower than the value of 7.04 kJ m^{-2} determined from the impact tests.

5. Conclusions

The fracture toughness of injection-moulded short glass fibre-reinforced thermoplastic nylon 6.6 plaques was measured under the static and the impact loadings. The influences of specimen position as taken from plaques mouldings, notch direction, rate of testing and notch sharpness on the fracture toughness of this composite system were studied. Results indicated that the fracture toughness is highest for cracks perpendicular to the mould fill direction and for this crack direction the measured value of the fracture toughness is not affected by the sharpness of the initial notch and the average fracture toughness is 10.36 MPa $m^{1/2}$. However, for cracks in the mould fill direction, the sharpness of the initial notch had a significant effect upon the measured value of fracture toughness. For razor-notched specimens, the average fracture toughness was 6.00 MPa $m^{1/2}$ which is considerably lower than the value of 7.97 MPa $m^{1/2}$ obtained using saw cuts. Furthermore, the fracture toughness for this composite material was found to be rate insensitive over the crosshead speed ranging from 0.5–50 mm min^{-1} ($K_{c,L\text{-cracks}}$ = 6.02 MPa $m^{1/2}$ and $K_{c,T\text{-cracks}}$ = 9.71 MPa $m^{1/2}$). Finally, results indicated that the specimen position has no significant effect on the measured value of the fracture toughness.

Acknowledgement

The authors thank Dr B. A. Crouch, Dupont de Nemours and Company Inc, for the provision of the materials for this study.

References

1. K. FRIEDRICH, *Plastics Rubber Process. Applic.* **3** (1983) 255.
2. D. C. LEACH and D. R. MOORE, *Composites* **16** (1985) 113.
3. J. F. MANDELL, A. Y. DARWHISH, and T. J. McGARRY, ASTM STP 734 (American Society for Testing and Materials, Philadelphia, PA, 1981) p. 73.
4. W. F. BROWN, J. E. STRAWLEY, ASTM STP 410 (American Society for Testing and Materials, Philadelphia, PA, 1966) p. 12.
5. ASTM E399-78a, "Standard Test Method for Plane Strain Fracture Toughness of Metallic Materials", 1979 Annual Book of ASTM standards, Part 10 (American Society for Testing and Materials, Philadelphia, PA, 1979) p. 540.
6. E. ROBERTS, Jr, *Mater. Res. Standards* **9**(2) (1969) 27.
7. G. P. MARSHALL, J. G. WILLIAMS and C. E. TURNER, *J. Mater. Sci.* **8** (1973) 949.
8. S. HASHEMI and J. G. WILLIAMS, *ibid.* **19** (1984) 3746.
9. J. A. NAIRN, ICCM & ECCM, "Sixth International Conference On Composite Materials, and Second European Conference On Composite Materials", Vol. 3, July 1987, p. 3.200.

Received 4 September 1991
and accepted 9 January 1992